Polymer Chemistry

Accepted Manuscript

This is an *Accepted Manuscript*, which has been through the Royal Society of Chemistry peer review process and has been accepted for publication.

Accepted Manuscripts are published online shortly after acceptance, before technical editing, formatting and proof reading. Using this free service, authors can make their results available to the community, in citable form, before we publish the edited article. We will replace this *Accepted Manuscript* with the edited and formatted *Advance Article* as soon as it is available.

You can find more information about *Accepted Manuscripts* in the Information for Authors.

Please note that technical editing may introduce minor changes to the text and/or graphics, which may alter content. The journal's standard Terms & Conditions and the Ethical guidelines still apply. In no event shall the Royal Society of Chemistry be held responsible for any errors or omissions in this *Accepted Manuscript* or any consequences arising from the use of any information it contains.

ROYAL SOCIETY OF CHEMISTRY

www.rsc.org/polymers

Journal Name

RSCPublishing

ARTICLE

Sequential two-stage polymerization to synthesis isotactic polypropylene/isotactic polybutene-1 alloys: compositions, morphologies and granule growing mechanism

Cite this: DOI: 10.1039/x0xx00000x

Received 00th January 2012,
Accepted 00th January 2012

DOI: 10.1039/x0xx00000x

www.rsc.org/

Baiyu Jiang, Huafeng Shao, Huarong Nie and Aihua He*

In this paper, a crystalline/crystalline polyolefin alloy - isotactic polypropylene/ isotactic polybutene-1 (iPP/iPB) in-reactor alloys with spherical particle morphology, were synthesized by sequential two-stage polymerization using spherical $MgCl_2$-supported Ziegler-Natta catalyst. The achieved iPP/iPB alloys were mainly composed by isotactic polybutene-1, isotactic polypropylene and polypropylene-*block*-poly(butene-1) block copolymers, which occupied more than 95 wt% of the total alloy. The possible polymerization mechanism was proposed to explain the block copolymer formation. The morphologies of original alloy particles and n-heptane-extracted alloy particles were characterized by SEM and a particle growth model of iPP/iPB alloy was proposed to illustrate the sequential two-stage polymerization mechanism and active-specie distribution during this process.

Introduction

Polyolefin materials, as the most widely used materials in real life, had attracted lots of attentions during the past 20 years. Especially, the progresses of the olefin polymerization catalysts had driven and accelerated the development of polyolefin materials. In 1953-1954, Ziegler-Natta catalysts were discovered and the realized stereoregularity polymerizations of α-olefin broke the monopoly of nature synthesis.[1] Significantly, every progress in Ziegler-Natta catalyst definitely led to the huge progress in productivity and stereoregularity, as shown in Table 1.[2,3] In 1982, Montell developed the Reactor Granule Technology (RGT) to synthesize the polyolefin in-reactor alloys based on the 4th generation Ziegler-Natta catalyst.[4] RGT was defined as: controlled, reproducible polymerization of olefinic monomers on an active magnesium chloride supported catalyst, to give a growing, spherical polymer granule that provides a porous reaction bed within which other monomers can be introduced and polymerized to form a polyolefin alloy.[5] This technology was a remarkable breakthrough in the development of high performance polyolefin materials. The typical polyolefin from RGT was PP (polypropylene)/EPR (ethylene-propylene copolymer rubber) in-reactor alloys.

Table 1 Milestones in PP catalyst development[2]

Generation	Composition and structure	Productivity[a] (kg·PP/g·Cat)	I.I. (wt%)
1st (1957-1970)	$TiCl_3/AlCl_3/AlEt_2Cl$	0.8-1.2	88-91
2nd (1970-1980)	$TiCl_3/AlEt_2Cl$	3-5 (10-15)	95
3rd (1978-1980)	$TiCl_4$/Ester/$MgCl_2$+ AlR_3/Silane	5-10 (15-30)	92
4th (1980) (Reactor Granule Technology) R.G.T	$TiCl_4$/Diester/$MgCl_2$+ TEA/Silane Three dimensional catalyst granule architecture.	10-25 (30-60)	98
	$TiCl_4$/Diether/$MgCl_2$+TEA Three dimensional catalyst granule architecture.	25-35 (70-120)	98

[a] Polymerization hexane slurry, 70 °C, 0.7 MPa, 4 hrs for M_w control (values in brackets are from bulk polymerization for 2 hrs at 70 °C, with H_2)

On the basis of RGT, the understanding of polymer particle growth mechanism has been an interesting subject both in the academic and industrial fields. The growth mechanism of polymer particle can be divided into two branches, one was the growth of iPP particle, and the other was the formation and distribution of EPR in the alloys. Till now, there were several theories and models[5-13] used to address the growth mechanism of iPP particles, but the formation and distribution of EPR was still in discussion.

Debling and Ray[14] and McKenna[15,16] *et al*. proposed that the EPR started to form underneath the iPP at the beginning of EPR formation stage. The build-up of pressure resulted from the presence of EPR caused the formation of cracks of iPP layer.

Meanwhile, the pressure caused by EPR formation led the rubber to flow out into the pore from the cracks. Du[17] *et al.* reported the same conclusion.
Kakugo[18] proposed that the EPR polymerized at the latter did not exist inside the subglobules, but in the boundary of the particles. Cecchin[19,20] *et al*. designed a series of experiments to prove that the catalyst fragments formed in the propylene polymerization stage were not in the interior of the polypropylene subglobules, but located at the surface. The EPR formed at the surface of the preformed homopolymer subglobules forming a polymer phase surrounding them and thus a continuous network within the host-homopolymer matrix. Chen[21] *et al.* also reported that the EPR did not form on the active sites within the primary particle, but only on the catalyst fragments distributed on the surface of the subglobules.
However, Urdampilleta[22] *et al.* insisted that most of EPR was finely dispersed inside the subglobules, but a few of the elastomers broke the polypropylene matrix and flowed to the voids between the subglobules.
Furthermore, most studies about granule growing mechanism were focused on the PP/EPR system, which was the plastic/rubber system or crystalline/elastomeric system. Consequently, the specific characteristics of EPR elastomer involved the low glass transition temperature, easy dissolution in monomer and easy flow, caused the difficulties in study of the granule growing mechanism. Moreover, the relatively low EPR content (less than 20 wt%) resulted from the diffusion control polymerization and active species embedding in PP/EPR system inhibit the further understanding of the granule growing mechanism.
In this paper, plastic/plastic system or crystalline/ crystalline system was used to address these issues instead of crystalline/elastomeric system. For this purpose, high isotactic polypropylene/high isotactic polybutene-1 (iPP/iPB) in-reactor alloys were synthesized by two stage sequential polymerization process with $MgCl_2$-supported Ziegler-Natta catalyst. As the typical crystalline/crystalline polymer blend system, iPP/iPB alloys with both high iPP content and high iPB content provided good models to study the polymer growth mechanism with supported Ziegler-Natta catalyst. The morphologies of iPP/iPB alloys were characterized by SEM and the iPP/iPB particle growth model was proposed to illustrate the sequential two-stage polymerization mechanism and active-specie distribution during this process. To the best of our knowledge, there were few literatures concerned about the plastic/plastic or crystalline/crystalline polymer blend system.

Experimental

Materials

Butene-1, propylene (polymerization grade, purity≥99.5%) and $MgCl_2$-supported Ziegler-Natta catalyst with 3.35 wt% titanium were kindly supplied by Orient Hongye Chemical Co. Ltd, (Shouguang city, Shandong province, China). Triethyl aluminium ($AlEt_3$) (>98% purity) was supplied by Yanshan Petrochemical Co. The n-heptane (analytical purity, Tianjin Guangcheng Chemical Factory) was refluxed continuously over sodium under nitrogen for 48 h, and distilled immediately before use. Other reagents were commercial product without further purification.

Synthesis of iPP/iPB in-reactor alloys

Sequential polymerizations were carried out in a 3 L stainless reactor. At the first polymerization stage, precise amount of n-heptane, $AlEt_3$, external electron donor and propylene at constant pressure were successively introduced into the reactor, and then the solid catalyst powder was added to start the propylene slurry polymerization at 60 °C for a constant polymerization time, and then the n-heptane and the unreacted propylene monomers were flashed completely with vacuum pump. Then, a certain amount of distilled liquid butene-1 was breathed into the reactor and the second polymerization was started at a constant temperature. The polymerization was quenched with ethanol containing 1% HCl solution and powdery products were washed with plenty of ethanol, filtered, and dried in a vacuum oven at 70 °C until the weight of the polymer was constant.

Fractionation of iPP/iPB in-reactor alloys

About 1 g of iPP/iPB in-reactor alloy was extracted with boiling diethyl ether in a Soxhlet extractor for 48 h. The diethyl ether soluble fraction was recovered by precipitation with acetone. The recovered diethyl ether soluble fraction and the diethyl ether insoluble fraction were vacuum dried overnight. Then the dried diethyl ether insoluble fraction was further extracted with boiling n-heptane in a Soxhlet extractor for 48 h. The n-heptane soluble fraction was recovered. Then the n-heptane soluble fraction and the n-heptane insoluble fraction were vacuum dried overnight. Finally， three fractions were obtained. The diethyl ether soluble fraction was named as A fraction, the n-heptane soluble fraction was named as B fraction and the n-heptane insoluble fraction was named as C fraction.

Characterization

^{13}C-NMR (100 MHz) measurement was carried out on a Bruker AVANCE III spectrometer at 105 °C with 1,2-dichlorobenzene-d4 as solvent. Delay time was 5 s, and typically 3000 transients were collected. Differential scanning calorimetry (DSC) analysis was made by a NETZSCH DSC-204 Differential Scanning Calorimeter under nitrogen atmosphere. The sample was heated from room temperature to 200 °C at a heating rate of 10 °C/min to eliminate the thermal history, and then cooled to room temperature at 10 °C/min. Then the samples were heated from room temperature to 200 °C at 10 °C/min, the heat flow versus time was recorded and the melting temperature was determined in the second scan. The morphology of iPP/iPB in-reactor alloys was observed using Jeol 7500F scanning electron microscope at an acceleration voltage of 1.0 kv. The melt flow rate (MFR) was measured on a GT-7100-MI melt flow rate testing instrument (GOTECH testing Machines Inc., Taiwan, China) with a 2.16 kg load at a test temperature of 190 °C according to GB/T3682-2000.

Results and discussion

Synthesis of iPP/iPB in-reactor alloys

Sequential two-stage polymerizations were adopted to synthesize a series of iPP/iPB alloys by changing the two stage polymerization time. Firstly, the active iPP particles were obtained in the first propylene polymerization stage. Then the unreacted propylene monomers and n-heptane were flashed completely by reducing pressure. Secondly, liquid butene-1 was breathed into the reactor and the active species in iPP particles began to initiate butene-1 polymerization. The polymerization

results of the synthetic iPP/iPB alloys with varied iPB content (26.7 ~ 91.6 wt%) were summarized in Table 2. Compared to our previous work, the biggest progress of this work was to provide the iPP/iPB alloys with very low A fraction content (lower than 4 wt%).

Table 2 summary of iPP/iPB alloys[a]

Samples	Polymerization time		Catalytic efficiency	Fractions (wt%)			MFR[b]
	First stage (min)	Second stage (h)	(kg·polymer/g·Ti)	A	B	C	(g/10 min)
iPB	0	5	297	2.4	97.6	0	0.35
alloy-1	1	1.5	50	2.0	91.6	6.4	0.53
alloy-2	1.5	2.5	55	2.8	80.0	17.2	0.64
alloy-3	12	4.5	68	2.5	72.0	25.5	0.60
alloy-4	20	5	73	2.4	67.6	30.0	0.64
alloy-5	120	7	64	3.5	26.7	69.8	1.18
alloy-6	22	7.5	61	3.4	47.2	49.4	0.10
alloy-7	10	7	61	1.5	80.2	18.3	0.25
iPP-1	40	0	35	3.6	0	96.4	9.34
iPP-2	40	0	45	3.9	0	96.1	1.47

[a] Polymerization condition: [Ti]/[butene-1] = 2 × 10^{-5} (mol/mol); [Al]/[Ti] = 80 (mol/mol); [D]/[Ti] = 10 (mol/mol); Propylene pressure = 0.4 MPa; n-heptane solvents = 100 mL; H_2 pressure: iPB = 0.02 MPa, iPP-1 = 0.015 MPa, iPP-2 = 0.005 MPa, alloy-1~alloy-4 = 0.015 MPa (first stage) and 0.02 MPa (second stage), alloy-5~alloy-7 = 0.005 MPa (first stage) and 0.02 MPa (second stage).

[b] Melt flow rate.

Compositions of iPP/iPB alloys

All the polymers were fractionated into A, B and C fractions, as shown in Table 2. In order to obtain the exact compositions in each fractions, alloy-4 was employed as an example, and ^{13}C-NMR and DSC were used to characterize the structures of A, B and C fractions.

As shown in Fig. 1, no melting peaks were observed for A fraction, indicating A fraction was amorphous polymer. The ^{13}C-NMR spectra of the A fraction showed no chemical shifts appeared at 43.03-43.51 ppm indicating no BP dyad sequence in A fraction[25] (Fig. 2a). However, chemical shifts at 46.00-46.95 ppm assigned to PP dyad sequences, and chemical shifts at 40.11 ppm assigned to BB dyad sequences were observed clearly. The enlarged chemical shifts from 9 to 11 ppm assigned to branched CH_3 of polybutene-1 (PB) and chemical shifts from 18 to 22 ppm assigned to branched CH_3 of polypropylene (PP) in Fig. 2a showed obviously that both PP and PB in A fraction were atactic polymers.[26] Therefore, it could be concluded that A fraction was not the random copolymers, but the blends of atactic polybutene-1 and atactic polypropylene.

As shown in Fig. 1, B fraction showed only one melting peak (around 114 °C), which could be attributed to the contribution of iPB. In Fig. 2b, four chemical shifts around 40.23, 35.01, 27.73 and 10.82 ppm were observed for B fraction, which were the characteristic chemical shifts of PB. The chemical shift at 27.73 ppm representing mmmm pentad sequences was very sharp and high. The absence of atactic chemical shifts indicated that the B fraction was highly isotactic (≥90 wt%) polymer. So the B fraction was composed by isotactic polybutene-1.

As shown in Fig. 1, C fraction showed two melting peaks, one was around 165 °C (T_m of PP) and the other was around 118 °C (T_m of PB) indicating C fraction might be composed by both PP and PB. ^{13}C-NMR spectra of C fraction in Fig. 2c also showed that the characteristic chemical shifts of both PB and PP. In addition, unique and obvious mmmm pentad sequences for both PP and PB segments were observed in Fig. 2c. Therefore, C fraction should be composed by iPP and polypropylene-*block*-poly(butene-1) block copolymer. The block copolymer made the iPB segments keep insoluble in boiling n-heptane extraction.

Therefore, it was concluded that alloy-4 was composed by 2.4 wt% atactic homopolymer, 67.6 wt% iPB and 30 wt% iPP and polypropylene-*block*-poly(butene-1) block copolymer. The iPP/iPB alloy was a highly isotactic polymer. The isotacticity of the alloy was higher than 97 wt%. The high isotacticity for both PP and PB will constitute a crystalline/crystalline polymer alloy. The quick crystallization of iPB will push the iPB chains into stackings and the shrinked space will provide void for the next monomer coordination and chain propagation. So the easy crystallization behaviour of iPB will make it to possible prepare iPP/iPB alloy with super high iPB content, and also provide a good model to study the particle growing mechanism.

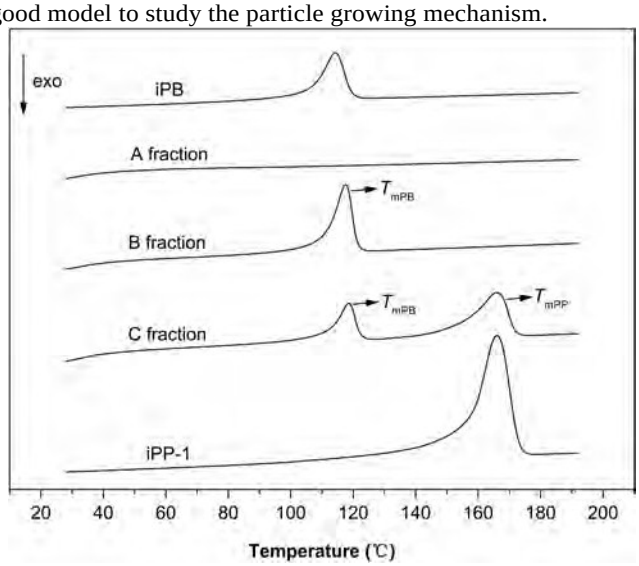

Fig. 1 DSC endothermal curves of alloy-4

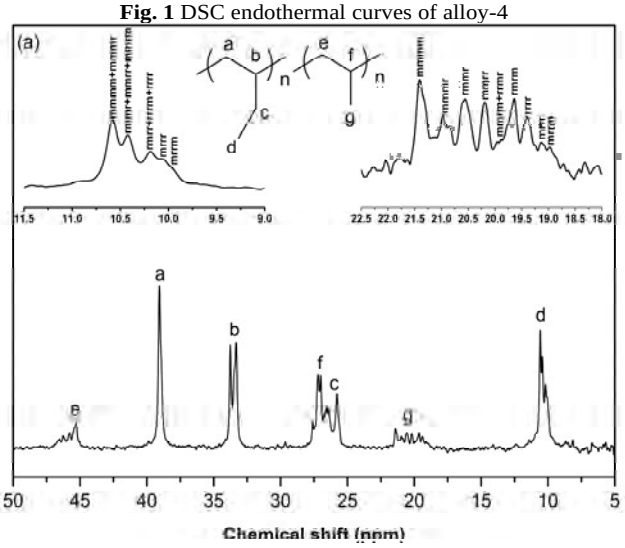

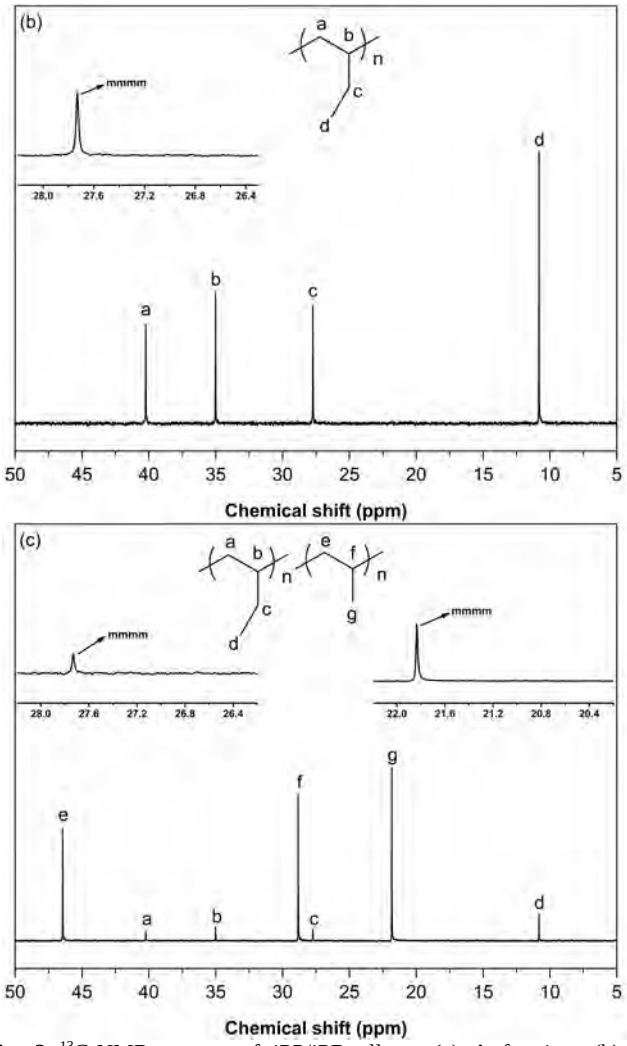

Fig. 2 ^{13}C-NMR spectra of iPP/iPB alloys: (a) A fraction; (b) B fraction; (c) C fraction.

Mechanism for the formation of different components in iPP/iPB alloys

The mechanism for the formation of the different components in iPP/iPB in-reactor alloys were depicted in Scheme 1. As a molecular weight regulator, hydrogen was widely used in coordination polymerization. In the first propylene polymerization stage, the propylene coordinated with Ti (III) active species to form the propagation chain active species (Ti-PP) by successive addition of the propylene monomers. Simultaneously, during the chain propagation, hydrogen may react with the Ti-PP as chain transfer agent, and dead PP chains and new active species (Ti-H) were formed. At the end of the first stage, all unreacted propylene monomers, hydrogen and solvent were flashed by reducing pressure with vacuum pump. Then butene-1 monomers were introduced to start the second polymerization with hydrogen as the molecular weight regulator. The pre-existed two kind active species including Ti-H and Ti-PP initiated the butene-1 polymerization. Ti-H active species produced PB, while Ti-PP chain active species coordinated with butene-1 monomers and further formed Ti-PP-*block*-PB active species. During the chain propagation, hydrogen may react with the Ti-PP-*block*-PB as chain transfer agent and form dead polypropylene-*block*-poly(butene-1) block copolymers and new active species (Ti-H). Ti-H active species will continue initiating the polymerization of butene-1 to form PB.[27] Finally, iPB, iPP and polypropylene-*block*-poly(butene-1) block copolymers were produced. A few atactic active species would lead to less than 4 wt% atactic homopolymers.

Morphology of iPP/iPB alloys before and after extraction

The morphology of the supported Ziegler-Natta catalyst was characterized by SEM. As shown in Fig. 3, the supported Ziegler-Natta catalyst presented spherical particle morphology, and lots of pores with pore size in the range of 1-1000 nanometers were observed on the rough surface. The porous structure of the supported catalyst could provide access for the monomers easily diffusing into the interior of the catalyst during the polymerization process.

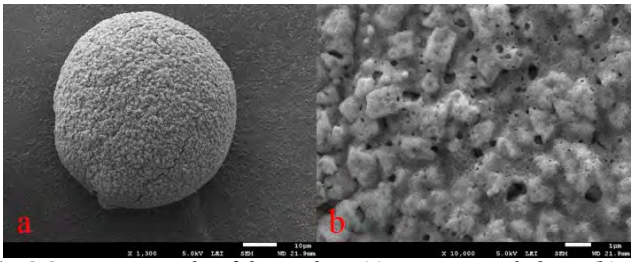

Fig. 3 SEM micrographs of the catalyst: (a) pristine morphology; (b) external surface.

Fig. 4A ~ E showed the particle morphology of the iPP/iPB alloys. It could be observed that the alloy particles replicated the morphology of the catalyst[28] and also presented very beautiful spherical morphologies. Differently, the surface of the iPP/iPB alloy was smooth. It was desirable for polymer particles with regular and spherical shape in view of preventing reactor fouling problems and undesirable fluidization effects.[29] The particle surface morphologies were shown in Fig. 4F ~ J. As shown in Fig. 4F, the surface of iPP particle was rough and porous. While the surface of iPB particle was relatively smooth (Fig. 4J). For iPP/iPB in-reactor alloys, with the incorporation of butene-1 upon the iPP matrix, the surface of the particles became smoother, suggesting that the iPB component filled in the pores of the iPP particles as shown in Fig. 4G, H and I. After the solvent extraction, the iPB fraction was removed, the particle surface of the alloys became coarse and porous obviously as shown in Fig. 4f, g and h. Furthermore, as shown in Fig. 4a ~ d, after extraction by boiling n-heptane, the size of alloy-7 (iPB-80.2 wt%) and alloy-6 (iPB-47.2 wt%) decreased greatly.

In order to obtain more information of the internal porous structure of the particles, iPP and alloy particles were cut into two pieces by using a razor blade. One side was directly observed by SEM. The other side was extracted with boiling n-heptane to ensure the soluble iPB fractions were removed completely, and then, observed by SEM. It could be seen that the iPP particles were composed by thousands of globules (Fig. 5F), whereas the iPB and alloy particles showed smooth surface and the enlarged images showed no obvious sub-structures. Therefore, the results supported the point that the iPB components filled the pores outside of the iPP subglobules.

Fig. 5a and e showed that the internal structure of the iPP particles was not affected by the extraction and obvious iPP subglobules could be observed. Compared to the pristine alloy-5 particles, it seemed that both the size of the extracted alloy particles with lower iPB content (26.7wt%, Fig. 5b) and the size of the iPP subglobules (Fig. 5f) changed a little.

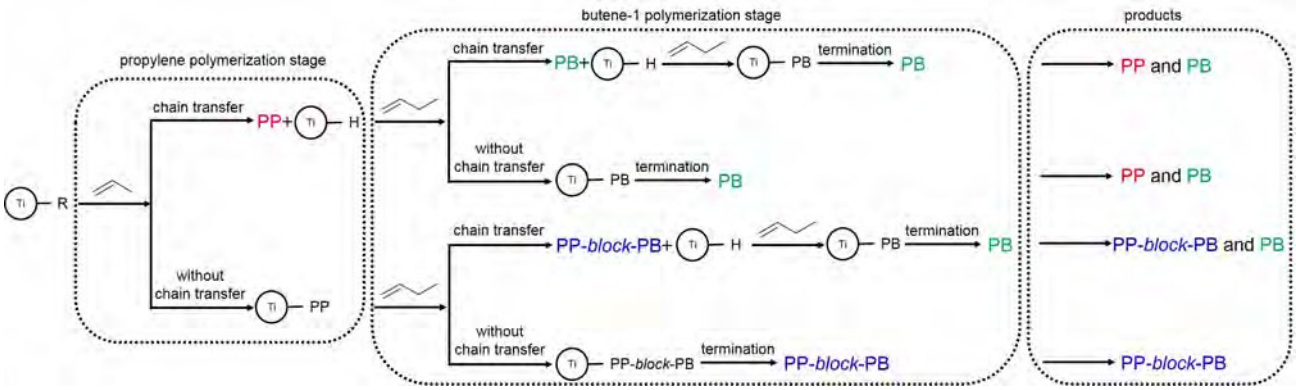

Scheme 1 Formation of the different components of iPP/iPB in-reactor alloys.

Therefore, it can be concluded that iPB were firstly polymerized inside the iPP particle but outside the iPP subglobules. However, compared to the pristine alloy particles, the size of the extracted alloy particles with higher iPB content (Fig. 5c and Fig. 5d) decreased a lot, and after extraction, the iPP subglobules were obvious as shown in Fig. 5 g and Fig. 5h. It seemed that the polymerized iPB enveloped the iPP particle.

Possible mechanism of the growth of iPP/iPB alloys

According to the aforementioned analysis and based on the following three hypothesises, possible schematic model for the particle growth of iPP/iPB in-reactor alloys was illustrated in scheme 2. The first hypothesis was that both iPP and iPB crystallized at corresponding polymerization temperature in the reactor to form solid. The second hypothesis was that the crystallization rate of iPP was very fast and could provide enough pressure to crack the catalyst. The third hypothesis was that the crystallization rate of iPB was slower than iPP and crystallized iPB might be in form II with lower melting temperature and was not hard enough to cause the crack of iPP. The crystallization of iPB will push the iPB chains into stackings and the shrinked space will provide void for the next butene-1 monomer coordination and chain propagation. So the easy crystallization behaviour of iPB will make it possible to prepare iPP/iPB alloy with super high iPB content and also provide a good model to study the particle growing mechanism. Therefore, at the propylene homopolymerization stage, the porous catalyst particles were burst into fragments by the growing polypropylene and formed a polymer shell around each fragment. These fragments were held together by the intermingling of the polymer chains.[17] As polymerization proceeded, catalyst likely underwent further fragmentation and the effective catalysts tended to locate on the surface of iPP subglobules. Cecchin[20] *et al.* had proved this phenomenon through relevant experiments. At the butene-1 polymerization stage, it seemed that most catalyst active species were existed inside the iPP particles and therefore iPB were formed on the boundary of the iPP subglobules. Due to the slow crystallization of iPB and relatively soft form II crystals, the preformed iPB could not build-up pressure to crack iPP particles. When the voids inside iPP particles were filled completely, some active species transferred to the iPP particle surface and continued to initiate the butene-1 polymerization. Therefore the latter formed iPB will enwrap the iPP particle as shell layers with the further polymerization.

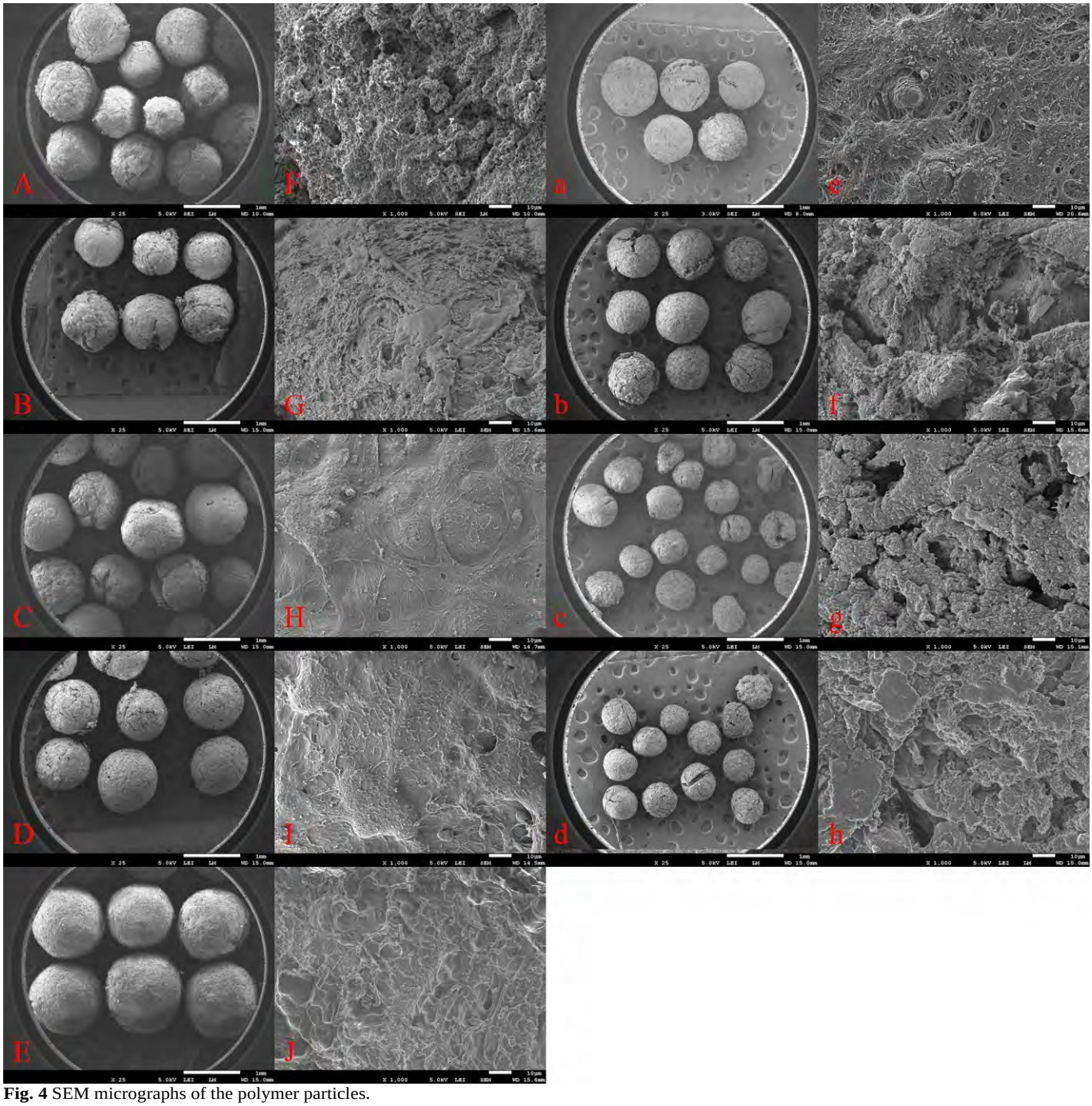

Fig. 4 SEM micrographs of the polymer particles.
(A) ~ (E) were the pristine morphologies of the particles: (A) iPP-2; (B) alloy-5; (C) alloy-6; (D) alloy-7; (E) iPB.
(F) ~ (J) were the enlarged morphologies of the particles: (F) iPP-2; (G) alloy-5; (H) alloy-6; (I) alloy-7; (J) iPB.
(a) ~ (d) were the morphologies of the particles after extraction with boiling n-heptane: (a) iPP-2; (b) alloy-5; (c) alloy-6; (d)alloy-7.
(e) ~ (h) were the enlarged morphologies of the particles after extraction with boiling n-heptane: (f) iPP-2; (g) alloy-5; (h) alloy-6; (i) alloy-7.

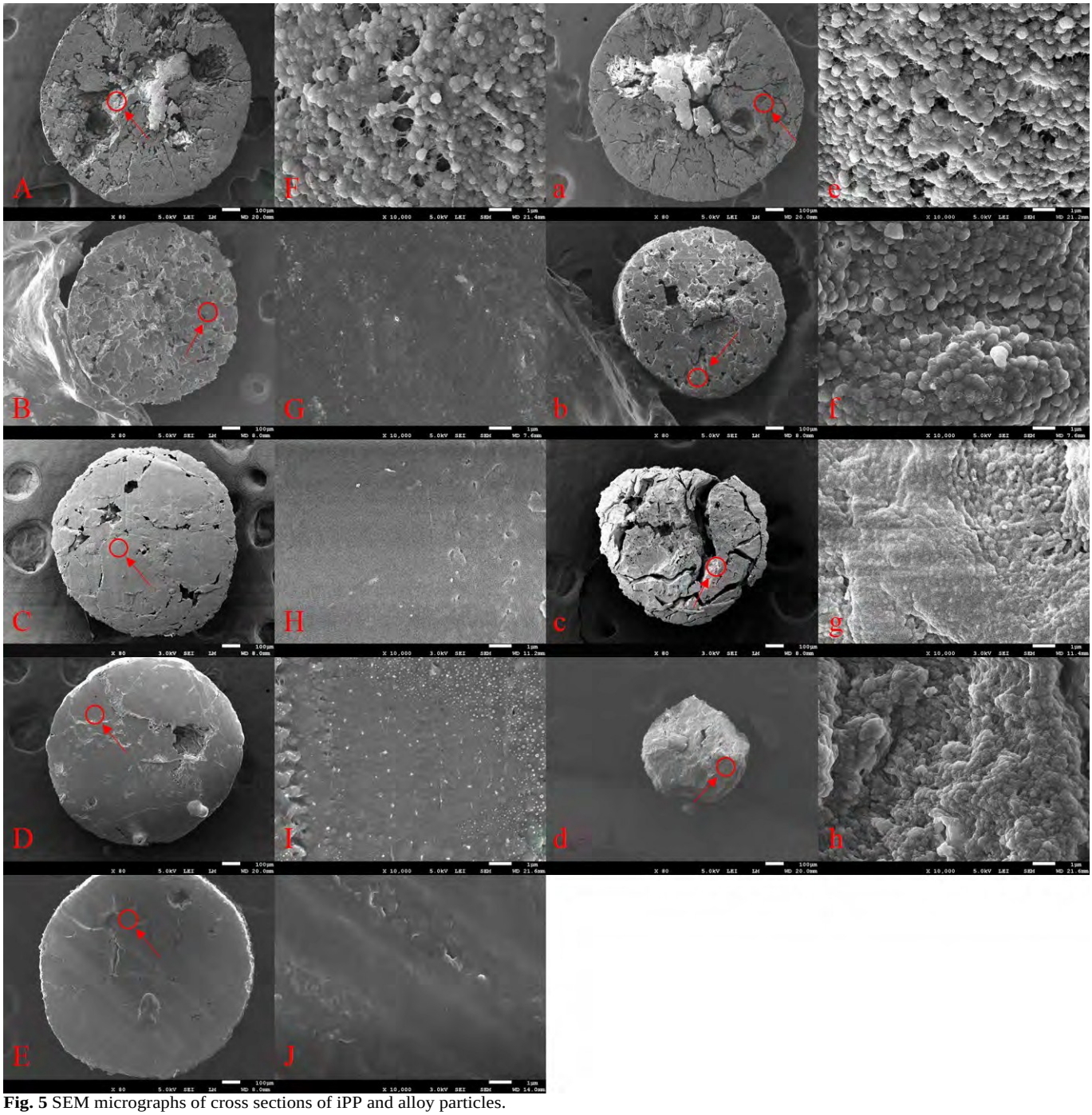

Fig. 5 SEM micrographs of cross sections of iPP and alloy particles.
(A) ~ (E) were the images of cross sections of pristine particles: (A) iPP-2; (B) alloy-5; (C) alloy-6; (D) alloy-7; (E) iPB.
(F) ~ (J) were enlarged images from the circled areas in (A) ~ (E), respectively.
(a) ~ (d) were the images of cross sections of particles after extraction with n-heptane: (a) iPP-2; (b) alloy-5; (c) alloy-6; (d) alloy-7.
(e) ~ (h) were enlarged images from the circled areas in (a) ~ (d), respectively.

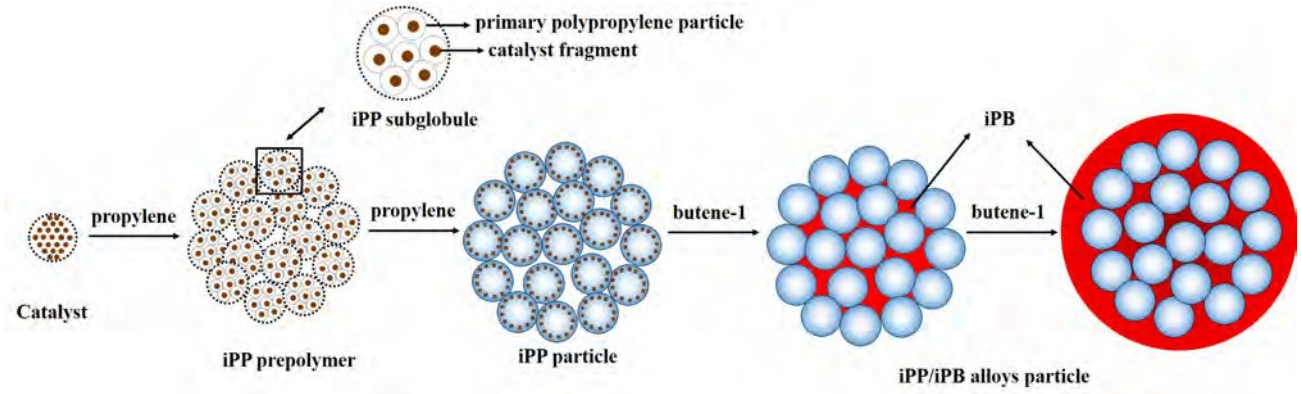

Scheme 2 Proposed model of the particle growth of iPP/iPB in-reactor alloy

Conclusions

The iPP/iPB in-reactor alloys, prepared by sequential two stage polymerization, were mainly composed of isotactic polybutene-1, isotactic polypropylene, polypropylene-*block*-poly(butene-1) block copolymers, and a little amount of atactic polymers including polybutene-1 and polypropylene. The iPP/iPB were composed by about 97 wt% isotactic polymers. The iPP/iPB alloys showed spherical particles, and iPB formed the outer layers when iPB content was more than 50 wt%. The possible mechanism of the particle growth of iPP/iPB alloys was illustrated as followed: Firstly, the porous catalyst particles were burst into fragments by the growing polypropylene at the propylene homopolymerization stage and iPP particles were formed consisted by lots of iPP subglobules. As polymerization proceeded, catalyst likely underwent further fragmentation and the effective catalysts tended to locate on the surface of iPP subglobules. Secondly, at the butene-1 polymerization stage, iPB were formed on the boundary of the iPP subglobules, once the voids inside iPP particles were filled completely by iPB, the active species transferred to the iPP particle surface and continued to initiate the butene-1 polymerization. Therefore the latter formed iPB will enwrap the iPP particle as shell layers.

Acknowledgements

This work was financially supported by the Shandong Province Natural Science Fund for Distinguished Young Scholars (JQ201213), the National Nature Science Foundation of China (No.21174074), National Key Technology R&D Program of China (2011BAE26B05), and the Nature Science Foundation of Shandong Province (ZR2013BN004).

Notes and references

Key Laboratory of Rubber-Plastics，Ministry of Education / Shandong Provincial Key Laboratory of Rubber-Plastics, School of Polymer Science and Engineering, Qingdao University of Science and Technology, Qingdao 266042, China. E-mail: aihuahe@iccas.ac.cn; Fax: +86-0532-84022951; Tel: +86-0532-84022951.

1 X. Jiang, A. He. *Polym. Int.*, 2014, **63**, 179.
2 P. Galli. *J. Macromol. Sci., Pure Appl. Chem.*, 1999, **A36**, 1561.
3 P. Galli, G. Vecellio, in Organometallic Catalysts and Olefin Polymerization, ed. R. Blom, A. Follestad, E. Rytter, M. Tilset and M. Ystenes, Springer, Berlin Heidelberg, 2001, ch. 3, pp. 169-195.
4 P. Galli. *Prog. Polym. Sci.*, 1994, **19**, 959.
5 P. Galli, J. Haylock. *Macromol. Chem., Macromol. Symp.*, 1992, **63**, 19.
6 R. Hutchinson, C. Chen, W. Ray. *J. Appl. Polym. Sci.*, 1992, **44**, 1389.
7 M. Kakugo, H. Sadatoshi, J. Sakai, M. Yokoyama. *Macromol. Chem. Phys.*, 1988, **189**, 2589.
8 M. Kakugo, H. Sadatoshi, M. Yokoyama, K. Kojima. *Macromolecules*, 1989, **22**, 547.
9 M. Kakugo, H. Sadatoshi, J. Sakai, M. Yokoyama. *Macromolecules*, 1989, **22**, 3172.
10 M. Ferrero, R. Sommer, P. Spanne, K. Jones, W. Conner. *J. Polym. Sci., Part A: Polym. Chem.*, 1993, **31**, 2507.
11 M. Ferrero, E. Koffi, R. Sommer, W. Conner. *J. Polym. Sci., Part A: Polym. Chem.*, 1992, **30**, 2131.
12 L. Noristi, E. Marchetti, G. Baruzzi, P. Sgarzi. *J. Polym. Sci., Part A: Polym. Chem.*, 1994, **32**, 3047.
13 R. Hutchinson, C. Chen, W. Ray. *J. Appl. Polym. Sci.*, 1992, **44**, 1389.
14 J. Debling, W. Ray. *J. Appl. Polym. Sci.*, 2001, **81**, 3085.
15 P. Kittilsen, T. Mckenna. *J. Appl. Polym. Sci.*, 2001, **82**, 1047.
16 T. McKenna, D. Bouzid, S. Matsunami, T. Sugano. *Polym. React. Eng.*, 2003, 11, 177.
17 J. Du, H. Niu, J. Dong, X. Dong, C. Han. *Adv. Mater.*, 2008, **20**, 2914.
18 M. Kakugo, H. Sadatoshi, J. Sakai. *Stud. Surf. Sci. Catal.*, 1990, **56**, 345.
19 G. Cecchin, G. Morini, A. Pelliconi. *Macromol. Symp.*, 2001, **173**, 195.
20 G. Cecchin, E. Marchetti, G. Baruzzi. *Macromol. Chem. Phys.*, 2001, **202**, 1987.
21 Y. Chen, Y. Chen, W. Chen, D. Yang. *Polymer*, 2006, **47**, 6808.
22 I. Urdampilleta, A. Gonzalez, J. Iruin, J. Cal, J. Asua. *Macromolecules*, 2005, **38**, 2795.

23 A. He, W. Zheng, Y. Shi, G. Liu, W. Yao, B. Huang. *Polym. Int.*, 2012, **61**, 1575.
24 A. He, Y. Shi, G. Liu, W. Yao, B. Huang. *Chin. J. Polym. Sci.*, 2012, **30**, 632.
25 F. Silva, E. Lima, J. Pint, T. McKenna. *Macromol. Chem. Phys.*, 2005, **206**, 2333.
26 T. Asakura, M. Demura, Y. Nishiyama. *Macromolecules*, 1991, **24**, 2334.
27 J. Xu, L. Feng. *Polym. Int.*, 1998, **47**, 433.
28 J. Wang, H. Niu, J. Dong, J. Du, C. Han. *Polymer*, 2012, **53**, 1507.
29 F. Machiado, E. Lima, J. Pinto, T. McKenna. *Eur. Polym. J.*, 2008, **44**, 1130.